Japan Bilingual Publishing Co.

New Environmentally-Friendly Materials

https://ojs.bilpub.com/index.php/nefm

ARTICLE

A New Eco-Friendly Approach for Smart Composite Structures Based on Carbon Nanotube Fibres

Brahim Attaf

Independent Researcher in Composite Materials and Structural Engineering, 13013, Marseille, France

ABSTRACT

In the global nanocomposites market, carbon nanotubes (CNTs) are gaining significant attention due to their potential for revolutionary, high-performance applications. However, proactive measures are still required to ensure their safe use across the entire life cycle, minimizing environmental and health risks. To address these challenges and meet sustainability goals and ecodesign standards, this paper proposes a balanced, eco-friendly approach based on a key performance indicator (KPI), referred to as the ecological factor (eco-factor). This eco-factor will integrate environmental, health, and quality considerations across all stages of the life-cycle assessment, including material selection, characterization testing, theoretical modelling, finite-element analysis, manufacturing processes, maintenance and repair strategies, material recovery and recycling, and energy consumption. By promoting a transparent regulatory framework, well-defined safety requirements, and a stable legal environment, this approach aims to enhance the global competitiveness of future CNT-reinforced nanocomposites in the fields of nanotechnology and advanced materials. With this idea as an objective, our techno-scientific approach could become a normative tool for qualification and certification of future eco-products based on CNT materials, thus guaranteeing their sustainability in terms of economic, environmental and societal conditions. Furthermore, eco-technological action constitutes our primary objective for the coming years and will be pursued through the development of new regulatory requirements, codes, and ecological standards that promote safe and sustainable production within a circular

*CORRESPONDING AUTHOR:

Brahim Attaf, Independent Researcher in Composite Materials and Structural Engineering, 13013 Marseille, France; Email: b.attaf@wanadoo.fr

ARTICLE INFO

Received: 3 June 2025 | Revised: 4 October 2025 | Accepted: 12 October 2025 | Published Online: 19 October 2025
DOI: https://doi.org/10.55121/nefm.v4i2.746

CITATION

Attaf, B., 2025. A New Eco-Friendly Approach for Smart Composite Structures Based on Carbon Nanotube Fibres. New Environmentally-Friendly Materials. 4(2): 27–42. DOI: https://doi.org/10.55121/nefm.v4i2.746

economy framework. This approach is expected to enhance the competitiveness of CNT-based composite companies committed to implementing effective environmental management systems.

Keywords: Carbon Nanotube-Based Composites; Eco-Friendly Nanomaterials; Nanotechnology; Sustainable Development; Environmental Assessment; Health Protection; Quality Assurance

1. Introduction

In today's era of rapid advancement and remarkable innovation in materials science, fibre-reinforced composite materials have become key enablers in the development of structural components and technical devices that continue to enhance the health, comfort and quality of human life. Currently, recent advances in nanotechnology have enabled the development of a new class of continuous fibres based on carbon nanotubes (CNTs). These CNT fibres are envisioned as potential alternatives to conventional fibres due to their ultra-high-performance indices and exceptional physicochemical properties. Such advantages locate CNTs as promising reinforcements for next-generation composite structures and devices. In addition, CNTs exhibit significant potential as integrated sensing elements, allowing real-time monitoring of structural health and enabling control over both static and dynamic structural responses. Within the global composites market, these nanomaterials are attracting growing interest for a wide range of innovative and high-impact applications. Nevertheless, comprehensive regulatory frameworks remain essential to ensure that their development, deployment, and end-of-life management do not pose adverse environmental or human health risks.

Sundar et al.[1] presented a review article summarizing the standard methods used for carbon nanotubes and their application in drug delivery for cancer treatment. Whereas Arumugam et al.[2] have presented a recent development on the integration of CNTs into sustainable agriculture, offering a transformative opportunity to increase crop productivity while mitigating environmental damage. Sallakhniknezhad and his collaborators[3] have examined the applications of CNTs in improving the mechanical characteristics of cutting tools, including increasing wear resistance, strength and thermal conductivity, thus extending tool life and performance.

1.1. Comparison of Specific Strength and Specific Stiffness in Common Materials

The widespread use of these smart materials is believed to be linked to the good performance indices in terms of stiffness-to-weight ratio (E/ρ), also referred to as specific stiffness, and strength-to-weight ratio (σ/ρ)[4], also referred to as specific strength, and other extraordinary physicochemical properties, which are not achievable with conventional materials such as optical properties, thermal and electrical conductivities[5–8]. The ultra-high-performance indices of CNTs compared to other composite reinforcement materials are shown in **Figure 1**[9].

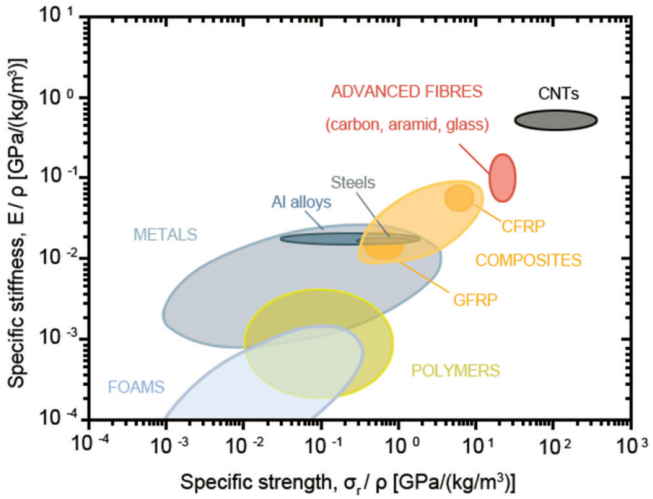

Figure 1. Specific strength vs. specific stiffness for some commonly used materials[9].

For instance, the strength of these fibres can be several times greater than that of conventional carbon fibres, while their weight is significantly lower for an equivalent cross-sectional area. However, despite these remarkable intrinsic properties, ecological uncertainties persist, and it is essential to address them to enable a realistic assessment of potential environmental and health impacts [10].

1.2. Similarities Between Asbestos and CNTs: Impact on the Human Body

With this great innovation, significant improvements and challenges can be achieved within the next generation of continuous fibre-reinforced composites based on CNT technology. However, recent medical research has shown that carbon nanotube (CNT) fibres share several similarities with asbestos fibres (see **Figure 2**) and may interact with the human body in a comparable manner. Specifically, CNT fibres could affect internal organs in ways analogous to asbestos, potentially leading to respiratory issues and mesothelioma: a deadly form of lung cancer that may not manifest until 30 to 40 years after exposure [11–16].

In response to this challenge, environmentally conscious designers must consider the environmental impacts of their products and identify alternative solutions to enhance product competitiveness in the global polymer nanocomposite market.

To address this question and comply with the requirements of the REACH (Registration, Evaluation, Authorisation and Restriction of Chemicals) regulation [17], a key parameter within the ecodesign strategy (hereafter referred to as the *eco-factor*) was developed through the application of probability theory and the integration of the three primary dimensions of sustainable development. These dimensions are addressed by systematically considering environmental, health, and qualitative aspects at each stage of the design process [18]. Collectively, this approach aims to deliver CNT-based composite products that are healthier, safer, cleaner, and more sustainable.

Therefore, adopting this contemporary approach can greatly enhance the advancement of these nanomaterials and can also help boost the level of potential development for a variety of high-performance applications [19,20].

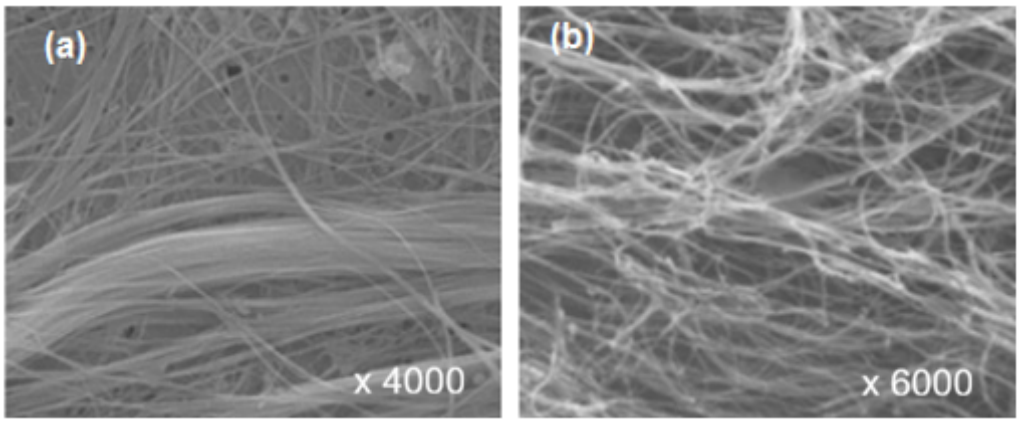

Figure 2. Microscopic view of fibres: (**a**) asbestos; (**b**) CNTs [16].

2. Structure and Chirality of Carbon Nanotubes

This discovery led to the development of single-walled carbon nanotubes (SWCNTs) and multi-walled carbon nanotubes (MWCNTs), which vary in chirality and geometry (e.g., zigzag, armchair, and chiral). These structures are poised to be integral to the development and fabrication of next-generation nanocomposites for high-performance applications across engineering, electronics, and medicine [21]. Depending on their atomic arrangement and chirality, carbon nanotubes (CNTs) may exhibit metallic or semiconducting electronic properties. These characteristics have enabled the creation of intelligent materials and innovative products at the nanoscale, with the potential to become integral to daily life by enhancing the performance, efficiency, and functionality of technologies across a wide range of sectors, including aerospace, electronics, biomedical engineering, energy stor-

age, and environmental sustainability.

Looking ahead, the development of CNT-based materials guided by eco-friendly approaches[10] could provide a foundation for future standards in the qualification and certification of nanocomposite products in the global market.

2.1. Chirality of CNTs

The geometry of a carbon nanotube is defined by the cutting plane of the graphene sheet relative to the coordinate frame (O; $\vec{a}_1$, $\vec{a}_2$) within the hexagonal carbon lattice, as illustrated in **Figure 3**[16]. Using the chiral vector ($\vec{C}_k = n \cdot \vec{a}_1 + m \cdot \vec{a}_2$), carbon nanotubes are categorized into three configurations: armchair ($n = m$), zigzag ($m = 0$), and chiral ($n \neq m$). Each configuration corresponds to a distinct arrangement of carbon atoms along the nanotube axis, influencing its electronic and mechanical properties.

Depending on their geometrical configurations, carbon nanotubes (CNTs) can exhibit either metallic or semiconducting electrical properties, as determined by their indices (n, m). Armchair configurations are always metallic, whereas zigzag and chiral configurations can be either metallic or semiconducting. These configurations are metallic when the condition $n - m = 3p$, where p is a natural integer ($p \in \mathbb{N}$). This behaviour is illustrated in **Figure 3**, where red circles represent metallic CNTs and yellow circles represent semiconducting CNTs. It should be noted, however, that this rule applies only to CNTs with certain diameters, as significant curvature effects in small-diameter nanotubes can alter their electronic properties.

Carbon nanotubes (CNTs) are generally classified as either single-walled (SWNTs) or multi-walled (MWNTs). Their diameters ($d = \left\| \vec{C}_k \right\| / \pi$) vary depending on the structure: SWNTs typically range from 0.5 to 1.5 nm, whereas MWNTs usually exceed 100 nm[21–24].

At the nanoscale, optimizing the length-to-diameter ratio of carbon nanotubes (CNTs) becomes a critical design parameter. A higher ratio contributes significantly to improved load transfer, mechanical reinforcement, and interfacial bonding within CNT-based composite products, thereby enhancing their overall structural performance and long-term sustainability.

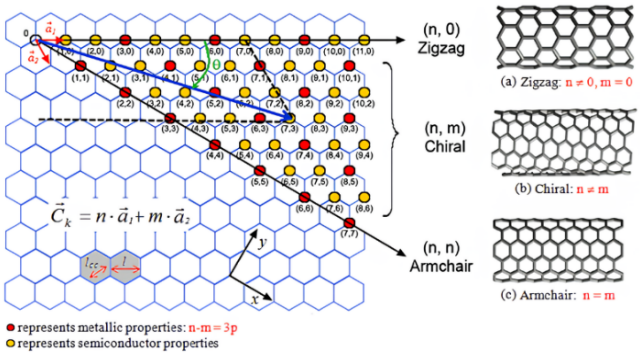

Figure 3. Chirality and symmetry of carbon nanotubes[16].

2.2. Geometric Formulations of CNTs

In the coordinate system (O; $\vec{a}_1$, $\vec{a}_2$) of the hexagonal lattice shown in **Figure 3**[16], the basic vectors $\vec{a}_1$ and $\vec{a}_2$ are expressed as[25,26]:

$$\vec{a}_1 = \begin{pmatrix} \frac{3}{2} \\ \frac{\sqrt{3}}{2} \end{pmatrix} l_{cc} \quad \vec{a}_2 = \begin{pmatrix} \frac{3}{2} \\ -\frac{\sqrt{3}}{2} \end{pmatrix} l_{cc} \tag{1}$$

where l_{cc} is the carbon–carbon bond length; equal to 0.1421 nm in graphite and slightly longer at 0.144 nm in carbon nanotubes due to curvature effects.

Since we know the norms of the two vectors $\|\vec{a}_1\| = \|\vec{a}_2\| = \sqrt{3}\, l_{cc} = l$, Equation (1) can be expressed in the Cartesian coordinate system (x, y) as:

$$\vec{a}_1 = \begin{pmatrix} \frac{\sqrt{3}}{2} \\ \frac{1}{2} \end{pmatrix} l \quad \vec{a}_2 = \begin{pmatrix} \frac{\sqrt{3}}{2} \\ -\frac{1}{2} \end{pmatrix} l \tag{2}$$

where l denotes the magnitude of the unit vector ($l = 0.2494$ nm).

When the chiral indices (m, n) are given, the chiral vector $\vec{C}_k$ and its magnitude (the nanotube circumference) are expressed as follows:

$$\begin{aligned} \overrightarrow{C}_k &= n \cdot \overrightarrow{a}_1 + m \cdot \overrightarrow{a}_2 \\ \left\| \overrightarrow{C}_k \right\| &= l\sqrt{n^2 + nm + m^2} \end{aligned} \tag{3}$$

Accordingly, the diameter of the nanotube, denoted by d_t, is defined as follows:

$$d_t = \frac{\|\vec{C}_k\|}{\pi} = \frac{l}{\pi}\sqrt{n^2 + nm + m^2} \tag{4}$$

Additionally, the chiral angle $\theta = (\overrightarrow{a}, \overrightarrow{C}_k)$ is defined by the following relation:

$$\theta = \tan^{-1}\left(\frac{\sqrt{3m}}{m\ +\ 2n}\right) \quad 0 \le |\theta| \le \frac{\pi}{6} \tag{5}$$

Likewise, the translation vector $\overrightarrow{T}$, which is perpendicular to the chiral vector, and its magnitude are given, respectively, by:

$$\begin{aligned} \vec{T} &= \frac{2m+n}{d_R}\vec{a}_1 - \frac{2n+m}{d_R}\vec{a}_2, \\ \|\vec{T}\| &= \frac{\sqrt{3}\|\vec{C}_k\|}{d_R} \end{aligned} \tag{6}$$

where $d_R = gcd\ (2n + m,\ 2m + n)$, and *gcd* denotes the greatest common divisor.

Finally, the number of hexagons in the nanotube unit cell, denoted by *N*, is given by:

$$N = \frac{2(n^2 + m^2 + nm)}{d_R} \tag{7}$$

3. Manufacturing Processes of CNTs

3.1. Chemical Vapor Deposition (CVD) Method for Nanomaterial Synthesis

Recent advances in cutting-edge synthesis techniques have enabled the development of a new class of continuous CNT-based fibres. Among these methods, chemical vapor deposition (CVD) has emerged as particularly promising, combining significant research potential with high scalability, which makes it highly attractive for industrial applications in the CNT sector.

The chemical vapor deposition (CVD) process involves a furnace supplied with a flow of carbon-containing gas, typically hydrocarbons (C_nH_m) such as acetylene (C_2H_2), diluted in a carrier gas like dinitrogen (N_2). The sample is positioned on a substrate holder made of materials such as silicon (Si), silicon dioxide (SiO_2), or quartz, which supports catalyst particles (e.g., Fe, Co, Ni, Pb) in the form of nanodroplets with diameters below 200 nm. Upon heating the furnace to approximately 750 °C, the catalyst particles facilitate the decomposition of acetylene, initiating the growth of carbon nanotubes (CNTs), which vertically extend within the quartz tube, forming an aligned "carpet" structure that can reach heights of several millimetres. The diameter of the CNTs corresponds closely to the size of the catalyst nanoparticles (nanodroplets).

The type of carbon nanostructure synthesized-single-walled (SWNT) or multi-walled carbon nanotubes (MWNT), is largely determined by the diameter of the catalyst particles. Catalyst particles with diameters around 1 nm predominantly yield SWNTs[27], whereas larger particles, typically between 10 and 50 nm, tend to produce MWNTs. Additionally, the number of walls in MWNTs generally increases with the catalyst particle diameter.

The growth rate of carbon nanotubes (CNTs) typically reaches up to 60 μm/min, but ongoing research and development efforts have enabled rates as high as 250 μm/min[28]. Furthermore, vertical alignment of CNTs (i.e., orientation perpendicular to the substrate surface) is achieved by applying an electric field, specifically via a negative polarization on the substrate[29]. **Figure 4** illustrates the mechanism of CNT growth using the chemical vapor deposition (CVD) technique.

Depending on the position of the catalyst particle, two distinct CNT crystal growth mechanisms (see **Figure 5**) can be employed in the CVD process to decompose the carbon-containing gas[30–32], namely:

- Base-growth mechanism: the catalyst nanoparticles remain anchored to the substrate during CNT growth (see **Figure 5b**).
- Tip-growth mechanism: the catalyst nanoparticles are lifted by the elongating CNTs, moving upward along with the nanotube (see **Figure 5c**).

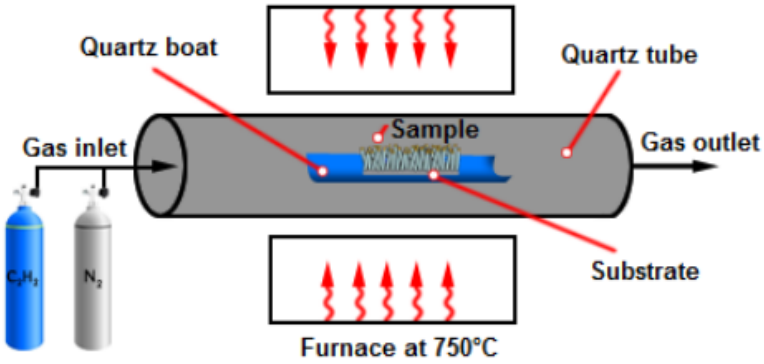

Figure 4. Schematic illustration of the CNT growth mechanism of the Chemical Vapor Deposition (CVD) process [16].

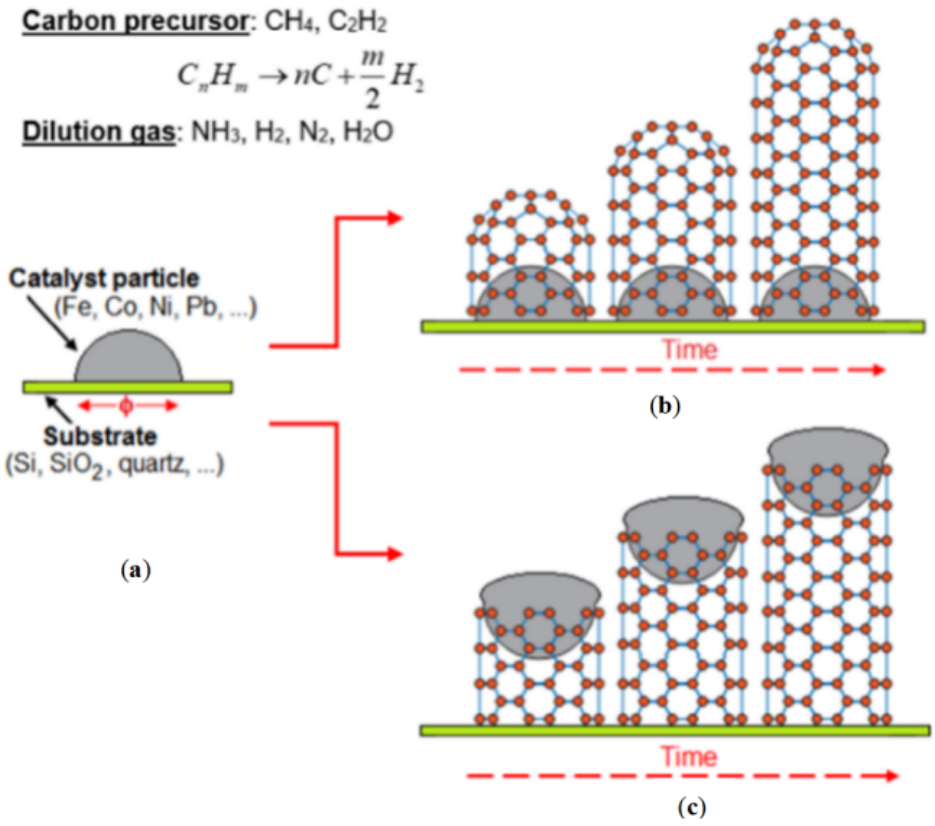

Figure 5. CNT growth mechanisms: (**a**) catalyst on substrate; (**b**) base-growth mechanism; (**c**) tip-growth mechanism [33].

In plasma-enhanced chemical vapor deposition (PECVD), a barrier layer-commonly silicon nitride (Si_3N_4) or a titanium nitride/silicon oxide (TiN/SiO_2) stack is introduced between the catalyst and the substrate. This barrier layer performs several critical functions [34], including:

- The assurance of good adhesion between the catalyst and the substrate.
- The prevention of reactions between the catalyst and substrate during CNT growth
- The guarantee of good electrical and mechanical contacts between the CNTs and the substrate.
- The good wettability of the catalyst in the liquid phase on the substrate surface, which ensures nanoparticle formation during the pre-growth phase.

Upon completion of the chemical reaction, the substrate wafer "typically silicon" is removed. Its surface is now covered with a dense array of vertically aligned carbon nanotubes (CNTs), forming a structure resembling a "toothbrush mat"

(see **Figure 6a**), with densities exceeding 10^9 CNTs/cm^2. Additionally, it is worth noting that adjacent CNTs exhibit unique interactions and interconnectivity, which can significantly influence their collective properties [35].

To produce CNT fibres, the process begins by gently pinching the end of a carbon nanotube and pulling it horizontally with a slight directional bias. This initial motion aligns adjacent nanotubes, which in turn pull neighbouring CNTs, initiating a self-sustaining chain reaction (see **Figure 6b**). During the subsequent spinning operation, the interconnected CNTs are twisted together to form a continuous, strong, and cohesive yarn. The mechanical strength of the resulting yarn is directly determined by the degree of twist applied. Finally, the continuous CNT yarn is wound onto a spool, producing a bobbin of aligned CNT-fibres, as illustrated in **Figure 6c**.

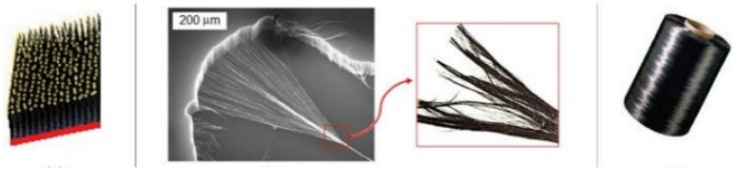

Figure 6. Manufacturing process of continuous CNT fibres: (**a**) vertically aligned CNT "carpet" on the substrate; (**b**) spinning of CNTs into a continuous fibre; (**c**) winding of the fibre onto a spool [36].

3.2. Lamination Technique Utilizing CNT Fibres

The resulting CNT fibres are woven into fabrics intended for the lamination process. These fibres can be aligned parallel to one another (unidirectional) or oriented at specific angles (bidirectional or multidirectional) to form tapes or fabrics. These materials, often referred to as semi-finished plies, consist of CNT fibres pre-impregnated with a polymer matrix. By stacking multiple dry or pre-impregnated plies in a pressure mould with varying fibre orientations, a finished composite structure, reinforced with continuous CNT fibres, is produced through closed-mould injection followed by curing of the thermoplastic resin. **Figure 7** illustrates the different length scales involved and highlights the key stages in the manufacturing process of this advanced nanocomposite material.

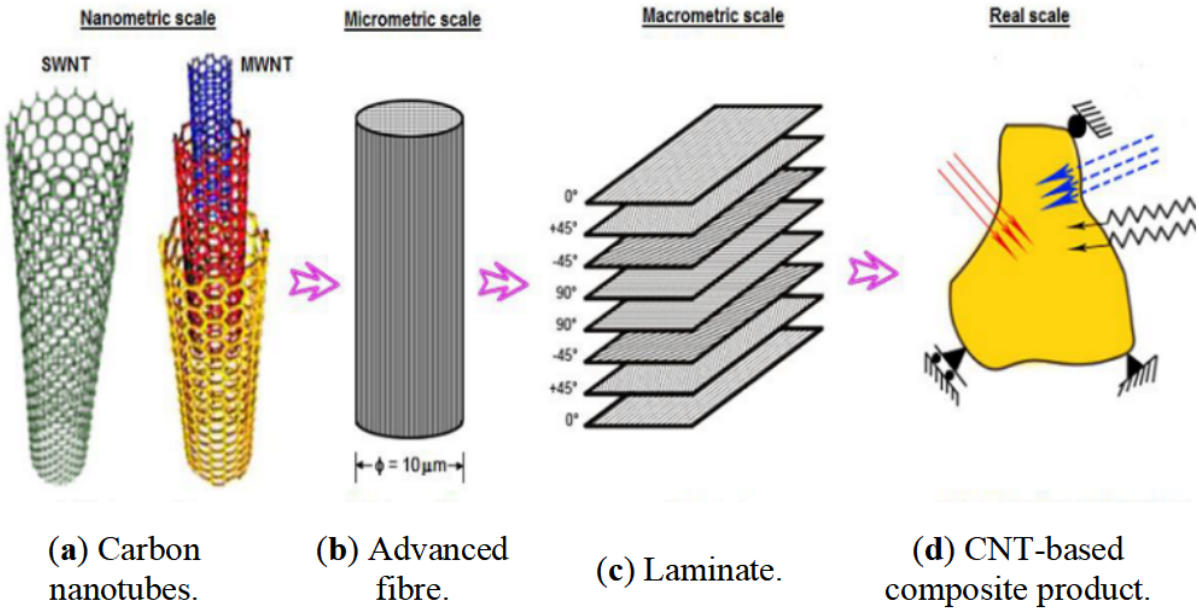

Figure 7. CNT fibres as reinforcement in next-generation nanocomposite structures [36].

3.3. CNT Properties vs. Traditional Fibres and Conventional Materials

Table 1 presents a comparison of the specific strength and specific stiffness of various materials, including conventional materials and individual fibres[8]. Within the category of fibre-reinforced composites, the relative positions of glass fibres, carbon fibres, and carbon nanotube (CNT) fibres can be clearly identified. The advantage of these advanced materials lies in their superior specific property ratios (performance indices), which are critical for meeting structural performance requirements while minimizing weight.

Table 1. Mechanical properties of some fibres and conventional materials vs. CNT fibres.

Fibres	Density (kg m^{-3})	Specific Stiffness E/ρ (MPa kg^{-1} m^3)	Specific Strength σ/ρ (MPa kg^{-1} m^3)
Glass E	2600	28.46	0.96
Carbon HS	1750	131.43	1.83
Kevlar 49	1450	89.65	2.00
Carbon HM	1800	216.67	1.39
Boron	2600	153.85	1.30
Steels	7800	26.28	0.05–0.2
Aluminium alloy	2800	26.78	0.16
CNT	1300–1400	770–3470	10–38

4. Innovative Eco-Friendly Model

Inspired by the Venn diagram concept[37–39], this investigation introduces an innovative eco-friendly model designed to assess and minimize environmental and health impacts, while ensuring full compliance with the relevant quality assurance standards for carbon nanotube composite materials.

The diagram presented in **Figure 8** illustrates the proposed eco-friendly model as an interaction among three key aspects: Quality (Q), Health (H), and Environment (E). These components form the foundation of the model and give rise to multiple subsets within the sample space[7]:

$$\Omega = \{Q, H, E, A, B, C, D, S, G, \dot{\dot{F}}, Ø\}$$

Among these subsets, only subset $\dot{\dot{F}}$ meets the criteria required for both ecodesign and sustainability. The three dots (.˙.) above the character F, symbolically refer to the diagram in **Figure 8**, which highlights the intersection of Q, H, and E (i.e., ∴). In this context, these dots represent the three pillars of sustainable development: environmental preservation, social well-being through health protection, and economic viability ensured by quality assurance.

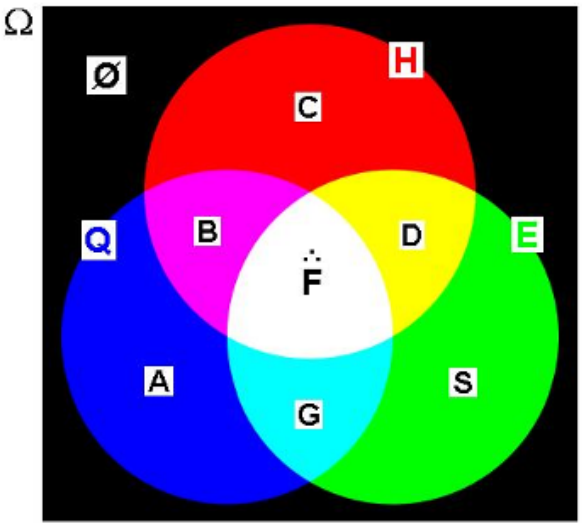

Figure 8. Attaf's eco-friendly model, inspired by the structure of a Venn diagram[10].

5. Formulating a Probabilistic Approach for Eco-Friendly CNT Materials

To assess the likelihood of achieving the desired event $\dot{\dot{F}}$, the concept of binomial probability is applied[40,41]. In this framework, the event and its associated probability can be mathematically expressed as follows:

$$\dot{\dot{F}} = Q \cap H \cap E \tag{8}$$

$$P(\dot{\dot{F}}) = P(Q \cap H \cap E) \tag{9}$$

where, $\cap$ denotes the intersection of sets.

According to the dependency relationships among the sets Q, H, and E, and using the multiplication rule from probability theory, Equation (9) may be formulated as:

$$P(\dot{\dot{F}}) = P(Q) \times P_Q(H) \times P_{Q\cap H}(E) \tag{10}$$

Since both the eco-friendly approach and the ecodesign process rely on the probability values defined in Equation (10), it is appropriate to assign each of the variables Q, H, and E a specific eco-coefficient, representing their respective probabilities of approval. Accordingly, we can express:

- $\alpha = P(Q)$: an eco-coefficient assessing the probability of approval in terms of *quality assurance*.
- $\beta = P_Q(H)$: an eco-coefficient assessing the probability of approval in terms of *health protection*, given that *quality assurance* has been achieved.
- $\gamma = P_{Q\cap H}(E)$: an eco-coefficient assessing the probability of approval in terms of *environmental preservation*, given that both *health protection* and *quality assurance* have been achieved.

The condition for "greening" the design and manufacturing processes, represented by the subset $\dot{\dot{F}}$ (see **Figure 8**), is evaluated by taking the mathematical product of the three eco-coefficients defined above. For simplicity, the resulting quantity is represented by a single variable, the *eco-factor*, denoted by the Greek letter λ. Using this simplified notation, Equation (10) can be rewritten as:

$$\lambda = \alpha \times \beta \times \gamma \tag{11}$$

The *eco-factor* λ is considered a key performance indicator (KPI), introduced here for the purpose of discussion, analysis, and evaluation. It serves as a tool to enhance life-cycle assessment (LCA) by integrating the interrelated aspects of Quality (Q), Health (H), and Environment (E) at each stage of the design and manufacturing processes.

For example, when the eco-factor λ approaches unity (i.e., 100%), it indicates full compliance with green design standards and sustainability criteria. Conversely, if λ falls significantly below the target threshold, it is recommended to explore alternative design strategies that yield improved eco-coefficients.

To facilitate clearer interpretation across different performance levels, **Table 2** summarizes the assessment process over defined intervals and presents a satisfaction rating using colour-coded indicators.

Table 2. Color-coded probability gauges for different eco-factor (λ) values[10].

Interval	Assessment	Gauge
$\lambda_5 \leq \lambda \leq 1$	Excellent	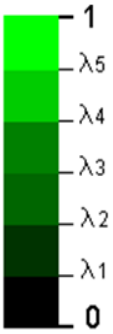
$\lambda_4 \leq \lambda < \lambda_5$	Very good	
$\lambda_3 \leq \lambda < \lambda_4$	Good	
$\lambda_2 \leq \lambda < \lambda_3$	Fair	
$\lambda_1 \leq \lambda < \lambda_2$	Poor	
$0 \leq \lambda < \lambda_1$	Very poor	

For instance, during theoretical and numerical analyses, the eco-factor λ will be incorporated into the standard mechanical characterization formulae for composite materials. As a result, the elastic moduli E_1, E_2, E_3 and shear moduli G_{12}, G_{23}, G_{13} of the unidirectional CNT-ply, as determined from experimental tests, are adjusted to account for the influence of the eco-factor, yielding updated values for these properties, namely: $\dot{E}_1$, $\dot{E}_2$, $\dot{E}_3$, $\dot{G}_{12}$, $\dot{G}_{23}$, $\dot{G}_{13}$.

In this context, for a unidirectional CNT-fibre/matrix ply, the updated engineering constants describing the linear-elastic mechanical behaviour can be defined in the principal coordinate system as follows[18]:

$$\dot{E}_i = \lambda E_i, \quad \dot{G}_{ij} = \lambda G_{ij}, \quad \text{with } \frac{\dot{E}_i}{\nu_{ij}} = \frac{\dot{E}_j}{\nu_{ji}} \qquad (i, j = 1, 2, 3 \text{ and } i \neq j) \tag{12}$$

where ν_{ij} is the classical Poisson's ratio for transverse strain in the *j*-direction when stressed in the *i*-direction. It should be noted that the updated values of Poisson's ratios were not investigated in relation to the eco-factor λ, as its influence falls beyond the scope of this analysis.

The structural analysis is illustrated in **Figure 9**. The isolated rectangular plate element is composed of multiple plies made of CNT fibres imbedded in thermoplastic matrix. As a result, the stacking sequence forms a thin laminated plate, where transverse shear deformation is neglected in accordance with Classical Lamination Theory (CLA).

When environmental, health and quality impacts are incorporated into the theoretical analysis, the constitutive relations for an unsymmetrically *k*-layered CNT laminated composite plate ($k = 1, 2, \ldots, n$) can be expressed in matrix form as follows[42,43]:

$$\begin{Bmatrix} N \\ \hline M \end{Bmatrix}_{xy} = \sum_{k=1}^{n} \int_{z_{k-1}}^{z_k} \begin{Bmatrix} \{\sigma\}_{xy} \\ \hline z\{\sigma\}_{xy} \end{Bmatrix} dz = \begin{bmatrix} \dot{A} & | & \dot{B} \\ - & - & - \\ \dot{B} & | & \dot{D} \end{bmatrix} \begin{Bmatrix} \varepsilon^0 \\ \hline \kappa \end{Bmatrix}_{xy} \tag{13}$$

where N and M denote the resultant in-plane forces and bending/torsional moments, respectively; and ε^0 and κ are the corresponding strains and curvatures.

Within this eco-friendly approach, the modified eco-stiffness components of the sub-matrices $\dot{A}_{ij}$ (eco-extensional), $\dot{B}_{ij}$ (eco-coupling) and $\dot{D}_{ij}$ (eco-bending) are expressed as:

$$(\dot{A}_{ij},\ \dot{B}_{ij},\ \dot{D}_{ij}) = \sum_{k=1}^{n} \int_{z_{k-1}}^{z_k} (\dot{\overline{Q}}_{ij})_k (1,\ z,\ z^2) dz \qquad (i, j = 1, 2, 6) \tag{14}$$

The ecologically durable components $\dot{\overline{Q}}_{ij} = \dot{\overline{Q}}_{ji}$ $(i, j = 1, 2, 6)$ are functions of the CNT-fibre orientation angle, θ, and the ply modified orthotropic elastic moduli.

With this objective in mind, the proposed approach facilitates a straightforward comparison between conventional results and sustainability-oriented results that incorporate the eco-factor λ. The percentage difference between these two result sets is referred to as the *eco-gap*, which can be quantified using the following formula:

$$\text{Eco-gap}(\%) = \left| \frac{V - \dot{V}}{V} \right| \times 100\% \tag{15}$$

where, $\dot{V}$ represents the sustainable result corresponding to $0 \leq \lambda < 1$, and V denotes the conventional result corresponding to $\lambda = 1$.

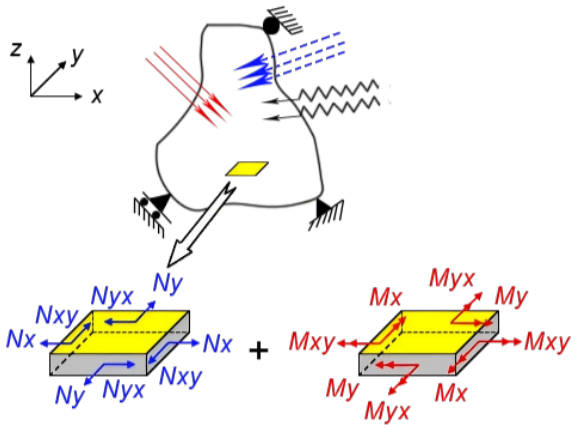

Figure 9. Diagram illustrating the internal forces and moments on the mid-plane of a thin plate element.

6. Results and Discussion

The ecodesign of a composite product reinforced with CNT-fibres involves a complex optimisation process that must simultaneously satisfy three key criteria: quality assurance (Q), health protection (H), and environmental preservation (E). Therefore, the development of a dedicated software tool is essential. The tool must be capable of addressing the associated probabilistic problems while employing advanced techniques to optimise both the ecodesign and manufacturing processes.

In this context, the optimisation process integrated within the software consists of three main stages:

1. **Identification and Data Collection**: This step determines the specific design stage (k = 1, 2, ...), collects the relevant data, and establishes the target probability value to be achieved.
2. **Analysis and Optimisation**: In this stage, the results are assessed and analysed with respect to the three criteria (Q, H, and E). If the initial outcomes do not meet the target, the software applies the optimisation procedure to achieve the desired probability threshold.
3. **Reporting and Reference Comparison**: In the final stage the software produces a specification sheet presenting the results of the eco-performance assessment. It also provides a comparative analysis with conventional (non-optimised) design solutions.

Using this multi-criteria approach, the key stages involved in assessing the sustainability of the CNT fibre-reinforced composite product are analysed step by step. They include:

- **Step 1:** Selection of raw materials and components including the polymer matrix and CNT fibre reinforcement.
- **Step 2:** Definition of the CNT fibre-reinforced composite material and formulation of the eco-design strategy.
- **Step 3:** Manufacturing and inspection of the first CNT fibre-reinforced composite prototype.
- **Step 4:** Qualification and certification of the first CNT fibre-reinforced composite product.
- **Step 5:** Launch of production across the supply chain.
- **Step 6:** Distribution and use of the CNT fibre-reinforced composite product.
- **Step 7:** Repair and maintenance of the CNT fibre-reinforced composite product.
- **Step 8:** End-of-life management of CNT fibre-reinforced composites, including recovery methods such as reuse, recycling, or energy recovery through incineration (conversion of waste into electrical or thermal energy).

It is important to note that each step (i = 1, ..., 8) is assigned an eco-factor λ_i, enabling a more detailed analysis of the results. The overall assessment of the sustainability performance of the CNT fibre-reinforced composite product can be expressed as follows:

- A 3 × 8 matrix containing the eco-coefficients α_i, β_i and γ_i (for i = 1, 2, ..., 8), which correspond respectively to quality assurance (Q), health protection (H), and environmental preservation (E) at each step.
- A 1 × 8 column matrix containing the probable results of all Q-H-E interactions in the form of eco-factors λ_i (i = 1, 2, ..., 8), as illustrated in **Figure 10**.

$$
\begin{array}{l}
 \\
\text{Step 1} \rightarrow \\
\text{Step 2} \rightarrow \\
\text{Step 3} \rightarrow \\
\text{Step 4} \rightarrow \\
\text{Step 5} \rightarrow \\
\text{Step 6} \rightarrow \\
\text{Step 7} \rightarrow \\
\text{Step 8} \rightarrow
\end{array}
\begin{array}{c}
\begin{array}{ccc} Q \downarrow & H \downarrow & E \downarrow \end{array} \\
\begin{bmatrix}
\alpha_1 & \beta_1 & \gamma_1 \\
\alpha_2 & \beta_2 & \gamma_2 \\
\alpha_3 & \beta_3 & \gamma_3 \\
\alpha_4 & \beta_4 & \gamma_4 \\
\alpha_5 & \beta_5 & \gamma_5 \\
\alpha_6 & \beta_6 & \gamma_6 \\
\alpha_7 & \beta_7 & \gamma_7 \\
\alpha_8 & \beta_8 & \gamma_8
\end{bmatrix}
\end{array}
\equiv
\begin{array}{c}
\textit{Eco-factor} \downarrow \\
\begin{bmatrix}
\lambda_1 \\ \lambda_2 \\ \lambda_3 \\ \lambda_4 \\ \lambda_5 \\ \lambda_6 \\ \lambda_7 \\ \lambda_8
\end{bmatrix}
\end{array}
$$

Figure 10. Illustrative matrix for the eco-friendliness assessment of CNT-reinforced composite products.

More specifically, this eco-friendliness approach can be illustrated through a graphical representation that displays the magnitude of each eco-coefficient on a normalized scale, while also highlighting the combined effect of the interrelated eco-coefficients by comparing the corresponding areas. Drawing inspiration from the normalized Kiviat diagram (spider chart), the distribution of the eco-coefficients α_i, β_i and γ_i (i = 1, 2, ..., 8) associated with the three key criteria—quality assurance (Q), health protection (H), and environmental preservation (E)—for a given step is illustrated in **Figure 11**.

By comparing the areas corresponding to the eco-factors λ_i (i = 1, 2, ..., 8), companies can efficiently and clearly evaluate the potential environmental and health impacts, as well as the quality assurance of their CNT fibre-reinforced composite products.

The optimisation process for each step is illustrated in the flowchart shown in **Figure 12**. The analysis conducted for stage i = 1 is subsequently repeated for the remaining steps in the design and manufacturing processes (i = 2…, N). For instance, if the final probability results approach unity, the objective is considered fully achieved; otherwise, alternative solutions must be explored.

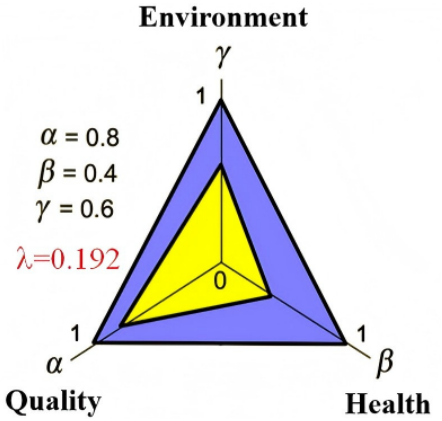

Figure 11. Diagram illustrating the distribution of eco-coefficients and the area proportional to the eco-factor λ [44].

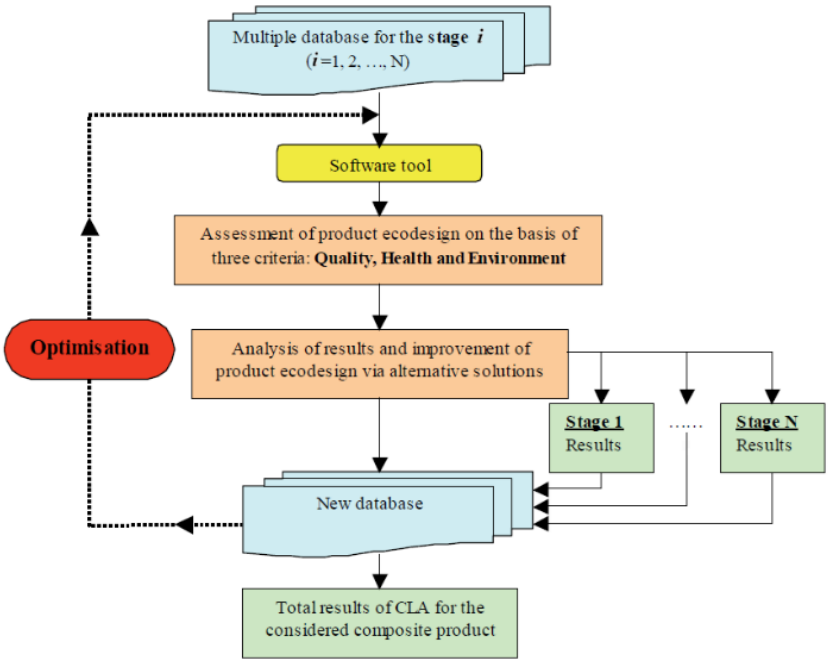

Figure 12. Process flowchart for ecodesign of CNT-based composite product.

To illustrate the optimisation procedure, consider a specific stage i in the design process, for example $i = 4$, corresponding to the "open mould polymerisation process." In this context, the quality assurance aspect and the health protection aspect, represented respectively by x_4 and y_4, are assumed to be both achievable and sustainable. However, the environmental preservation aspect, represented by z_4, is considered unachievable for this manufacturing process (i.e., open-mould polymerisation). Consequently, x_4 and y_4 belong simultaneously to the sets Q and H, placing them within subset B (i.e., $x_4 \in B$ and $y_4 \in B$), as illustrated in **Figure 13**. In contrast, z_4 does not belong to either Q or H ($z_4 \notin Q$ and $z_4 \notin H$), but is part of set E, and is therefore included in subset S.

To realize the desirable outcome, denoted by $\dot{\dot{F}}$, the element z_4 must be practically modified to ensure that the environmental preservation aspect becomes achievable and sustainable for "*closed-mould polymerisation process*". This is accomplished by transitioning from an open-mould to a closed-mould process. As a result, all three elements x_4, y_4, and z_4 associated with step 4 now satisfy the required criteria and are included in the relevant subset $\dot{\dot{F}}$, as illustrated in **Figure 13**. Further refinements may be applied to these elements to optimise performance and fully meet eco-friendly requirements.

As previously discussed, a similar transformation can be applied to other elements. For instance, let z_1 denote the statement: "environmental preservation aspect is unachievable for polyester resin with high-styrene content." This issue can be effectively addressed by replacing the high-styrene resin with a low-styrene alternative, yielding a revised z_1 that satisfies the condition: "the environmental preservation aspect is achievable for polyester resin with low-styrene content". This substitution aligns the new z_1 with the eco-friendly requirements.

The eco-factor calculated in this way can be integrated into mechanical characterisation tests, advanced mathematical models, and the constitutive equations of future CNT fibre-reinforced composite products. Moreover, by embedding this eco-factor within eco-friendly assessments that apply ecodesign and Life Cycle Assessment (LCA) principles, aligned with international standards such as ISO 14062 and ISO 14040, designers of CNT fibre-reinforced composites will benefit from enhanced validation criteria that comprehensively address environmental and health risks alongside quality assurance.

This integration will further promote the development of CNTs as an ideal reinforcement material for future composite products. However, critical questions regarding the threshold values of the eco-factor at each step remain undetermined. Future studies should address these issues to define precise acceptance and rejection intervals. Establishing such thresholds would allow for clearer assessments of compliance with emerging sustainability standards, which specify eco-factor limits. This currently missing element in existing standards could serve as a valuable reference for comparison, discussion, and continuous improvement.

The life-cycle analysis will comprehensively cover all stages across the entire value chain, with the goal of "closing the loop," as illustrated in **Figure 14**. A true circular economy approach can only be realized when all stages, including the extraction, transportation, and processing of raw materials, are considered as part of the loop [45]. By integrating these upstream processes, circular economy principles can be fully applied, ensuring that resources are used efficiently, waste is minimized, and the environmental impact is reduced across the entire product lifecycle. Moreover, the transition to a circular economy involves not only recycling and reusing materials but also redesigning products for longevity, repairability, and sustainability [46]. This approach fosters a more resilient and regenerative system, where resources flow continuously within the economy rather than being discarded after use.

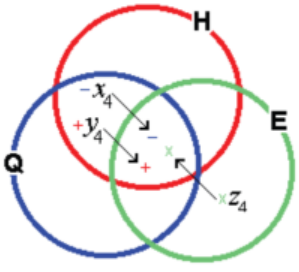

Figure 13. Example of an alternative solution related to step 4 [44].

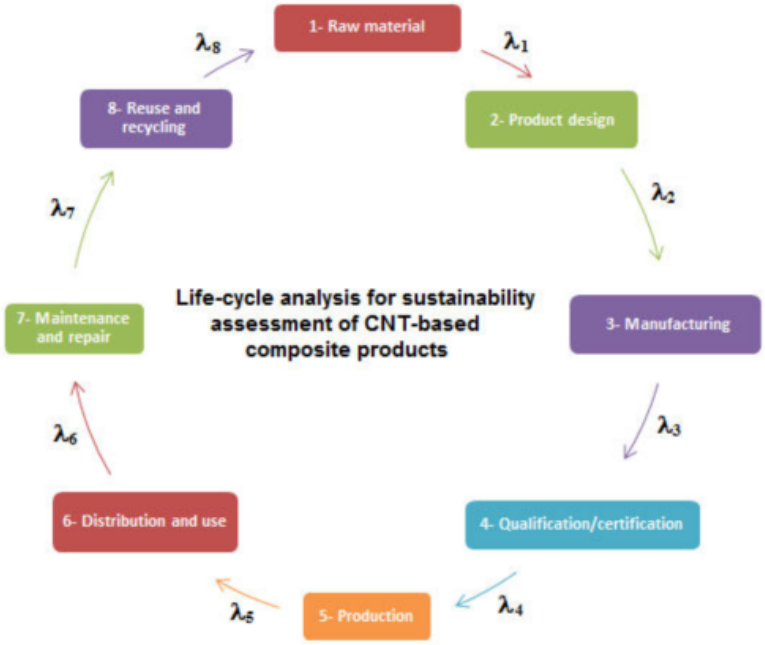

Figure 14. Life-cycle analysis for sustainability assessment of CNT fibre-reinforced composite products [44].

7. Conclusions

To meet eco-friendly requirements for future CNT-based composite products, this study developed a key eco-factor based on probability theory and integrated it with the three pillars of sustainable development. The work contributes to the advancement of international standards and promotes sustainable, health-conscious, and environmentally friendly design strategies. It provides a practical framework for companies to integrate quality, health, and environmental considerations across the life cycle of CNT fibre-reinforced composites, supporting circular economy principles.

Recommended best practices include careful selection and management of chemicals, reduction of VOC emissions, optimization of interrelated quality-health-environment (*Q-H-E*) issues, implementation of material recycling methods, and adoption of innovative approaches to comply with emerging regulations and eco-standards.

Funding

This work received no external funding.

Institutional Review Board Statement

Not applicable.

Informed Consent Statement

Not applicable.

Data Availability Statement

Not applicable.

Acknowledgments

The author gratefully acknowledges the reviewers for their valuable recommendations and insightful comments, which have substantially enhanced the quality of this article.

Conflicts of Interest

The author declares no conflict of interest concerning the content or conclusions of this independently conducted work. The study was carried out without any financial, personal, or professional relationships.

References

[1] Sundar, L.S., Djavanroodi, F., Apparao, T., 2025. Compatibility of Carbon Nanotubes for Biomedical Applications: A Review. Biomedical and Pharmacology Journal. 18(1), 431–446.

[2] Arumugam, A., Selvaraj, J.P., Palaniappan, T., 2025. Application of Carbon Nano Tubes for Sustainable Agriculture. International Journal of Research in Agronomy. 8(1), 564–568.

[3] Sallakhniknezhad, R., Ahmadian, H., Zhou, T., et al., 2024. Recent Advances and Applications of Carbon Nanotubes (CNTs) in Machining Processes: A Review. Journal of Manufacturing and Materials Processing. 8(6), 282.

[4] Wang, X., Yong, Z.Z., Li, Q.W., et al., 2013. Ultrastrong, Stiff and Multifunctional Carbon Nanotube Composites. Materials Research Letters. 1(1), 19–25.

[5] Radovic, L.R., 2002. Chemistry and Physics of Carbon: Volume 31. CRC Press: Boca Raton, FL, USA.

[6] Bradford, P.D., Bogdanovich, A.E., 2008. Electrical Conductivity Study of Carbon Nanotube Yarns, 3-D Hybrid Braids and Their Composites. Journal of Composite Materials. 42(15), 1533–1545.

[7] Zhu, Y., Qian, Y., Zhang, L., et al., 2021. Enhanced Thermal Conductivity of Geopolymer Nanocomposites by Incorporating Interface Engineered Carbon Nanotubes. Composites Communications. 24, 100691.

[8] Xu, W.H., Ravichandran, D., Jambhulkar, S., et al., 2021. Hierarchically Structured Composite Fibers for Real Nanoscale Manipulation of Carbon Nanotubes. Advanced Functional Materials. 31(14), 2009311. DOI: https://doi.org/10.1002/adfm.202009311

[9] Hart, J., 2009. Lecture 23 − Nanocomposites and Fibers. In ME 599: Nanomanufacturing. University of Michigan: Ann Arbor, MI, USA. Available from: http://www.infocobuild.com/education/audio-video-courses/mechanical-engineering/ME599-Winter2009-Umichi/lecture-23.html#google_vignette

[10] Attaf, B., 2007. Towards the Optimisation of the Ecodesign Function for Composites. JEC Composites. 34, 58–60.

[11] Ricaud, M., Lafon, D., Roos, F., 2008. Carbon Nanotubes: What Risks, What Prevention. INRS: Paris, France. pp. 43–57. (in French)

[12] Poland, C., Duffin, R., Kinloch, I., et al., 2008. Carbon Nanotubes Introduced into the Abdominal Cavity of Mice Show Asbestos-Like Pathogenicity in a Pilot Study. Nature Nanotechnology. 3, 423–428.

[13] Donaldson, K., Aitken, R., Tran, L., et al., 2006. Carbon Nanotubes: A Review of Their Properties in Relation to Pulmonary Toxicology and Workplace Safety. Toxicological Sciences. 92(1), 5–22.

[14] Muller, J., Huaux, F., Moreau, N., et al., 2005. Respiratory Toxicity of Multi-Wall Carbon Nanotubes. Toxicology and Applied Pharmacology. 207(3), 221–231.

[15] Du, J., Wang, S., You, H., et al., 2013. Understanding the Toxicity of Carbon Nanotubes in the Environment Is Crucial to the Control of Nanomaterials in Producing and Processing and the Assessment of Health Risk for Human: A Review. Environmental Toxicology and Pharmacology. 36(2), 451–462. DOI: https://doi.org/10.1016/j.etap.2013.05.007

[16] Attaf, B., 2015. Towards the Ecodesign Strategy for Automotive Components from Carbon Nanotube-Based Composites. International Journal of Automotive Composites. 1(4), 349.

[17] Commission of the European Communities, 2008. Communication From the Commission to the European Parliament, the Council and the European Economic and Social Committee. Regulatory Aspects of Nanomaterial. Commission of the European Communities: Brussels, Belgium. Available from: https://eur-lex.europa.eu/LexUriServ/LexUriServ.do?uri=COM:2008:0366:FIN:en:PDF

[18] Attaf, B., 2013. European Eco-Factor. Pan European Networks: Science and Technology. 7, 128–129.

[19] Hughes, K.J., Iyer, K.A., Bird, R.E., et al., 2024. Review of Carbon Nanotube Research and Development: Materials and Emerging Applications. ACS Applied Nano Materials. 7(16), 18695–18713.

[20] Nurazzi, N.M., Sabaruddin, F.A., Harussani, M.M., et al., 2021. Mechanical Performance and Applications of CNTs Reinforced Polymer Composites: A Review. Nanomaterials. 11(9), 2186.

[21] Zhang, Z., Zhang, N., Zhang, Z., 2025. High-Performance Carbon Nanotube Electronic Devices: Progress and Challenges. Micromachines. 16(5), 554.

[22] National Research Council, 2005. High-Performance Structural Fibers for Advanced Polymer Matrix Composites. The National Academies Press: Washington, DC, USA. Available from: http://www.nap.edu/catalog/11268

[23] Ganesh, E.N., 2013. Single Walled and Multi Walled Carbon Nanotube Structure, Synthesis and Applications. International Journal of Innovative Technology and Exploring Engineering. 2(4), 311–320.

[24] Malhotra, B.D., Srivastava, S., Augustine, S., 2015. Biosensors for Food Toxin Detection: Carbon Nanotubes and Graphene. Materials Research Society Symposium Proceedings. 1725, 24–34. DOI: https://doi.org/10.1557/opl.2015.165

[25] Maruyama, S., 2019. Chirality and Symmetry of Nanotube. Available from: http://www.photon.t.u-tokyo.ac.jp/~maruyama/kataura/chirality.html (cited 3 May 2020).

[26] Saito, R., Fujita, M., Dresselhaus, G., et al., 1992. Electronic Structure of Chiral Graphene Tubules. Applied Physics Letters. 60(18), 2204–2206.

[27] Soto, K.F., Carrasco, A., Powell, T.G., et al., 2005. Comparative In Vitro Cytotoxicity Assessment of Some Manufactured Nanoparticulate Materials Characterized by Transmission Electron Microscopy. Journal of Nanoparticle Research. 7(2–3), 145–169. DOI: https://doi.org/10.1007/s11051-005-3473-1

[28] Rao, C.N.R., Satishkumar, B.C., Govindaraj, A., et al.,

2001. Nanotubes. ChemPhysChem. 2, 78–105.

[29] Hata, K., Futaba, D.N., Mizuno, K., et al., 2004. Water-Assisted Highly Efficient Synthesis of Impurity-Free Single-Walled Carbon Nanotubes. Science. 306, 1362.

[30] Meyyappan, M., et al., 2003. Carbon Nanotube Growth by Plasma-Enhanced Chemical Vapor Deposition: A Review. Plasma Sources Science and Technology. 12, 205–216.

[31] Farmer, B.A., 2015. Modeling and Simulation of Carbon Nanotube Growth [PhD Thesis]. University of Michigan: Ann Arbor, MI, USA.

[32] Chen, X., Pang, X., Fauteux-Lefebvre, C., 2023. The Base Versus Tip Growth Mode of Carbon Nanotubes by Catalytic Hydrocarbon Cracking: Review, Challenges and Opportunities. Carbon Trends. 12, 100273.

[33] Attaf, B., 2021. Carbon Nanotube-Based Hybrid Composites in Drone Design Technology for Vaccination of Wild Animals. Asian Research Journal of Current Science. 3(1), 161–174.

[34] Leborgne, C., 2015. Growth of Carbon Nanotubes by PECVD: Example of an Application in Microelectronics. Available from: https://jrpf2016.sciencesconf.org/data/pages/Leborgne_Nanotubes.pdf (cited 14 April 2024). (in French)

[35] Fujimori, T., Yamashita, D., Kishibe, Y. et al. 2022. One Step Fabrication of Aligned Carbon Nanotubes Using Gas Rectifier. Scientific Reports. 12, 1285. DOI: https://doi.org/10.1038/s41598-022-05297-6

[36] Attaf, B., 2017. Composite Plates Based on Carbon Nanotube Fibres: Vibrations, Buckling, Delamination, Ecodesign and Durability. Editions Universitaires Européennes: Saarbrücken, Germany. (in French)

[37] Bartel, A.N., Lande, K.J., Roos, J., et al., 2021. A Holey Perspective on Venn Diagrams. Cognitive Science. 46(1), e13073. DOI: https://doi.org/10.1111/cogs.13073

[38] Yang, M., Chen, T., Liu, Y.-X., et al., 2024. Visualizing Set Relationships: EVenn's Comprehensive Approach to Venn Diagrams. iMeta. 3(3), e184. DOI: https://doi.org/10.1002/imt2.184

[39] Nakatsu, R.T., 2013. Using Venn Diagrams to Perform Logic Reasoning: An Algorithm for Automating the Syllogistic Reasoning of Categorical Statements. International Journal of Intelligent Systems. 29(1), 84–103. DOI: https://doi.org/10.1002/int.21628

[40] Collani, E.V., Drager, K., 2001. Binomial Distribution Handbook for Scientists and Engineers. Springer Nature: Berlin, Germany.

[41] Jia, Z., Du, Z., 2025. Decision-Making Research on Supply Chain Quality Inspection Based on Binomial Distribution and Monte Carlo Simulation. Academic Journal of Science and Technology. 14(2), 151–157. DOI: https://doi.org/10.54097/hyh43p61

[42] Jones, R.M., 1999. Mechanics of Composite Materials, 2nd ed. CRC Press: Boca Raton, FL, USA. DOI: https://doi.org/10.1201/9781498711067

[43] Saarela, O., 1994. Computer Programs for Mechanical Analysis and Design of Polymer Matrix Composites. Progress in Polymer Science. 19, 171–201.

[44] Attaf, B., 2015. An Eco-Approach to Boost the Sustainability of Carbon Nanotube-Based Composite Products. In Research and Innovation in Carbon Nanotube-Based Composites. World Academic Publishing: Singapore. pp. 1–13.

[45] Liu, L., Chang, D., Gao, C., 2024. A Review of Multifunctional Nanocomposite Fibers: Design, Preparation and Applications. Advanced Fiber Materials. 6, 68–105. DOI: https://doi.org/10.1007/s42765-023-00340-1

[46] European Parliament and Council of the European Union, 2024. Regulation (EU) 2024/1252 of the European Parliament and of the Council of 11 April 2024 establishing a framework for ensuring a secure and sustainable supply of critical raw materials and amending Regulations (EU) No 168/2013, (EU) 2018/858, (EU) 2018/1724 and (EU) 2019/1020. Available from: http://data.europa.eu/eli/reg/2024/1252/oj (cited 4 April 2025).